

Coherent transport in multi-branch quantum circuits

A. Ziletti,¹ F. Borgonovi,^{2,3} G. L. Celardo,^{2,3} F. M. Izrailev,^{4,5} L. Kaplan,⁶ and V. G. Zelevinsky⁵

¹*Dipartimento di Matematica e Fisica, Università Cattolica, via Musei 41, 25121 Brescia, Italy*

²*Dipartimento di Matematica e Fisica, Università Cattolica and Interdisciplinary Laboratories for Advanced Materials Physics, via Musei 41, 25121 Brescia, Italy*

³*I.N.F.N., Sezione di Pavia, Italy*

⁴*Instituto de Física, Universidad Autónoma de Puebla, Apartado Postal J-48, Puebla, Pue. 72570, México*

⁵*NSCL and Department of Physics and Astronomy, Michigan State University, East Lansing, Michigan 48824-1321, USA*

⁶*Department of Physics, Tulane University, New Orleans, Louisiana 70118, USA*

(Dated: March 7, 2022)

An open multi-branch quantum circuit is considered from the viewpoint of coherent electron or wave transport, both with and without intrinsic disorder. Starting with the closed system, we give analytical conditions for the appearance of two isolated localized states out of the energy band. In the open system, using the method of the effective non-Hermitian Hamiltonian, we study signal transmission through such a circuit, with an important result of a long lifetime of localized states. When the average level width becomes comparable to the mean level spacing, the super-radiant transition occurs. In the case of on-site disorder we find an analytical estimate, confirmed by numerical data, for the robustness of the isolated states and their role in transport processes.

PACS numbers: 05.20.-y, 05.10.-a, 75.10.Hk, 75.60.Jk

INTRODUCTION

The development of quantum informatics requires better understanding of the general problem of quantum signal transmission through discrete structures of interacting quantum elements, such as quantum dots [1–3], or molecular [4, 5] and Josephson junctions [6]. There is growing theoretical and experimental interest in arrangements more complicated than a simple one-dimensional chain, including Y- and T-shaped structures [7, 8], tetrahedral qubits [9], connected benzene rings [10], crossed chains [11], two- and three-dimensional lattices [12, 13], as well as graphs with the violation of time-reversal invariance at the junctions, supposedly with the aid of magnetic fields [14]. In all cases, one has to deal with a quantum system with intrinsic stationary states that become unstable when the system “opens” to the external world as a part of a transmission network.

The method of the effective non-Hermitian Hamiltonian, borrowed from nuclear physics [15], is a powerful and efficient tool for theoretical analysis of open quantum systems, as was shown by applications to one-dimensional structures [13, 16–20], covering both regular and chaotic internal dynamics; see the recent review of the method and its various adaptations [21]. In this work we consider the M -branch circuit in the form of $M > 2$ one-dimensional tight-binding chains with a common vertex at the central point. This system is a simple discrete example of quantum mechanics in a non-trivial space with self-crossings, singular points or surfaces where quasi-bound states (evanescent waves) may emerge even for open boundary conditions. Our interest is not only in the structure of the energy spectrum and eigenfunctions

for closed samples, which was earlier discussed for different purposes, see for example, the applications to Bose-Einstein condensation and temperature effects in optical networks [22], but mainly in the transport characteristics for the case when the chains are connected to an environment.

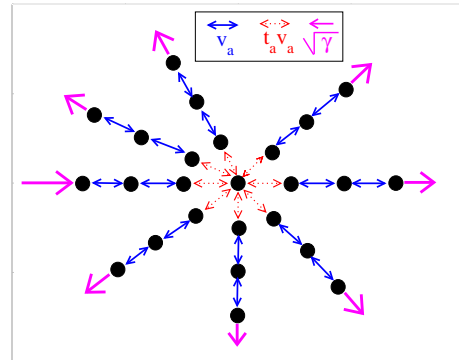


Figure 1: (Color online) The M -branch circuit with the coupling at the origin.

MODEL

We start with the discussion of the closed system and its energy spectrum. In our model (see Fig. 1), each of the M branches consists of N_a sites ($a = 1, \dots, M$) along which a particle/wave can propagate through the structure. The hopping amplitude v_a between nearest neighbor sites is constant within each branch, while the

coupling to the origin is given by $t_a v_a$. Thus, the Hamiltonian of the closed system is

$$\begin{aligned} \mathbf{H} = & \sum_{a=1}^M \sum_{n=1}^{N_a-1} v_a \left(|a, n\rangle \langle a, n+1| + |a, n+1\rangle \langle a, n| \right) \\ & + \sum_{a=1}^M t_a v_a \left(|0\rangle \langle a, 1| + |a, 1\rangle \langle 0| \right). \end{aligned} \quad (1)$$

In what follows, unless stated otherwise, we set $v_a = v$ and $N_a = N$, so that there are $K = MN + 1$ sites in total, including the vertex. The Schrödinger equation for a stationary state with energy E reduces to a set of algebraic equations for the site amplitudes C_n^a , where $a = 1, \dots, M$, and n labels the sites in each chain,

$$\sum_{a=1}^M t_a v C_1^a = EC_0; \quad v C_2^a + t_a v C_0 = EC_1^a;$$

$$v(C_{n-1}^a + C_{n+1}^a) = EC_n^a \quad \text{for } 2 \leq n \leq N, \quad (2)$$

with the boundary conditions $C_{N+1}^a = 0$.

SPECTRUM AND EIGENFUCTIONS

For $C_0 \neq 0$, the a -dependence of the amplitudes is given by $C_n^a = vt_a X_n$ with $n = 1, \dots, N$, while C_0 and the a -independent amplitudes X_n obey a tri-diagonal homogeneous set of $N + 1$ linear equations. The secular equation for $E \neq \pm 2v$ has the form,

$$(E^2 + E\epsilon_+ - v^2 Q)\epsilon_-^N - (E^2 + E\epsilon_- - v^2 Q)\epsilon_+^N = 0, \quad (3)$$

with the control parameter Q ,

$$Q = \sum_{a=1}^M t_a^2, \quad (4)$$

and $\epsilon_{\pm}(E) = (-E \pm \sqrt{E^2 - 4v^2})/2$. Note that for even N the value $E = 0$ is also a solution of Eq. (3). An analysis of Eq. (3) shows that the energy spectrum consists of a set of $MN - 1$ eigenvalues within the energy band $|E| < 2v$ (with eigenfunctions extended over the M branches of the circuit), and two additional eigenvalues with $|E| > 2v$, for sufficiently large M or sufficiently large couplings t_a .

We first consider the two states with the eigenvalues outside of the energy band (sometimes such states are called ‘‘hidden’’). These states turn out to be strongly localized at the origin of the circuit provided the parameter Q is large enough. In the limit $N \gg 1$, the energies of these states can be found from Eq. (3) by considering its largest and smallest roots. For $Q > 2$ one obtains

$$|\mathcal{E}_{\text{loc}}| = \frac{Q}{\sqrt{Q-1}} v, \quad (5)$$

which generalizes the results found in Refs. [23].

In order to find the structure of the corresponding eigenfunctions from Eq. (2), we obtain, after lengthy calculations, the following relation, valid for any finite N :

$$\left| \frac{C_{n+1}^a}{C_n^a} \right|^2 = \frac{1}{Q-1} \mathcal{B}_n(Q, N), \quad n = 1, \dots, N-1, \quad (6)$$

where we have defined the boundary factor,

$$\mathcal{B}_n(Q, N) = \left| \frac{1 - (Q-1)^{-(N-n)}}{1 - (Q-1)^{-(N+1-n)}} \right|^2, \quad (7)$$

which differs from 1 only for $n \approx N$. Neglecting for the time being this boundary effect (which however will be crucial for an open model, see below), we obtain

$$\left| \frac{C_n^a}{C_0} \right|^2 = \frac{t_a^2}{Q-1} e^{-(n-1)/\xi}, \quad n = 1, \dots, N; \quad Q > 2. \quad (8)$$

Here ξ is the localization length,

$$\xi = \frac{1}{\ln(Q-1)}, \quad (9)$$

of the two states outside the energy band, with the peak located at the origin of the circuit. Note that these states are spread over *all branches* in proportion to the couplings t_a^2 .

For $C_0 = 0$, one has standard extended Bloch states in each branch. However, the M solutions are linked through the first equation of (2), yielding $M - 1$ independent degenerate states for each $C_0 = 0$ eigenvalue. As a result, for the symmetric case of equal branch lengths $N_a = N$, we have two isolated localized states, N sets of $M - 1$ extended degenerate Bloch states with $C_0 = 0$, and $(N - 1)$ extended non-degenerate Bloch states with $C_0 \neq 0$, altogether $K = NM + 1$ states.

COUPLING TO CONTINUUM

Coming to the main goal of our study, now we consider the same circuit coupled to the environment by attaching the last site of each branch to an external channel, similarly to what has been done in Refs. [13, 16, 18, 20]. The open system is described by an effective non-Hermitian Hamiltonian [15, 21],

$$\mathcal{H} = \mathbf{H} - \frac{i}{2} \gamma \mathbf{W}; \quad \mathbf{W} = \sum_{a=1}^M A_N^a |a, N\rangle \langle a, N| A_N^{a*}. \quad (10)$$

Here \mathbf{H} is given by Eq. (1), while the coupling to the continuum via the ends of branches is characterized by the parameter γ and the matrix \mathbf{W} . The matrix \mathbf{W} is constructed out of the transition amplitudes A_N^a between intrinsic states $|a, N\rangle$ and continuum states $|a, E\rangle$. We

set $A_N^a = 1$, so that the strength of the coupling is controlled entirely by the parameter γ .

The lifetime τ_{loc} of the two localized states can be estimated via the imaginary part $-\Gamma_{\text{loc}}/2$ of the corresponding eigenvalues \mathcal{E}_{loc} of the complex Hamiltonian, $\tau_{\text{loc}} = \Gamma_{\text{loc}}^{-1}$. For small γ , the resonance width is determined by the spatial overlap of the localized states with the edges,

$$\Gamma_{\text{loc}} = \gamma \sum_{a=1}^M |\langle a, N_a | \psi_{\text{loc}} \rangle|^2, \quad (11)$$

see Refs. [15–17]. Taking into account Eqs. (6, 7, 9) with $|C_0|^2$ found from the normalization, for $N, Q \gg 1$ we have

$$\tau_{\text{loc}} = 2 \frac{(Q-1)^{N+1}}{\gamma Q(Q-2)} \simeq \frac{2}{\gamma} \exp\left(\frac{N-1}{\xi}\right). \quad (12)$$

Considering now the extended states inside the energy band, two different regimes can be distinguished [15, 16] as a function of γ . At weak coupling, all these states are similarly affected by the continuum coupling and acquire widths proportional to γ . For large γ , only M “super-radiant” states have a width proportional to γ , while the widths of the remaining (“trapped”) states fall off as $1/\gamma$. In order to find the critical value of the parameter γ corresponding to the super-radiant transition, we analyze the average value $\langle \Gamma \rangle$ of the $(MN+1) - M$ narrow widths as a function of the rescaled coupling γ/v . At a critical value γ_{cr} , the average width $\langle \Gamma \rangle$ peaks and begins to decrease.

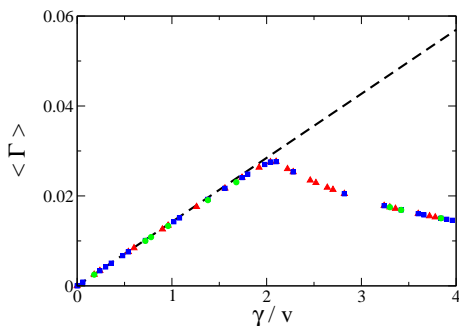


Figure 2: (Color online) The dimensionless average width $\langle \Gamma \rangle$ as a function of γ/v . We consider a) $M = 4$ and $N = 70$ with $t_a = 1$ for all branches (red triangles); b) $M = 4$ and $N = 70$ with different couplings $t_1 = 200$, $t_2 = 100$, $t_3 = 20$, and $t_4 = 50$ (blue squares); and c) $M = 4$ with different numbers of sites, $N_1 = 55$, $N_2 = 80$, $N_3 = 58$, $N_4 = 87$, and all $t_a = 1$ (green circles). The dashed line corresponds to the average over all widths, while the symbols are obtained by averaging over the $K - 4$ smallest widths, where $K = 281$ is the total number of sites in all cases.

One can evaluate γ_{cr} using the following criterion [16, 20]: the transition occurs when $\langle \Gamma \rangle$ becomes of the order of the mean level spacing D of the Hamiltonian

for the closed system. This is particularly easy for the special case of equal coupling $t_a = t$ and equal number of sites in each branch $N_a = N$; in this case it is convenient to define an effective mean level spacing as $D_{\text{eff}} \approx 4v/(2N+1) \simeq 2v/N$, which takes into account the level degeneracy. On the other hand, the average width is given by $\langle \Gamma \rangle \approx M\gamma/(MN+1) \simeq \gamma/N$, so that $\gamma_{\text{cr}} = 2v$ independently of M , N , and t_a . This result is numerically confirmed in Fig. 2, where it is shown to be valid even in the more general case of different coupling t_a and different number of sites N_a .

TRANSMISSION

Maximum transmission occurs at the super-radiant transition, as happens in one-dimensional chains [20]. Moreover the above analysis allows one to understand generic properties of the transmission between different branches. The data in Fig. 3 demonstrate the energy dependence of the transmission coefficient T_{ab} between two channels b and a . One can see that with an increase of γ the resonances corresponding to the energies from the bulk of spectrum begin to overlap, in contrast to the two very narrow resonances located out of the energy band. These quasi-bound resonances remain extremely stable even for a very strong coupling to continuum.

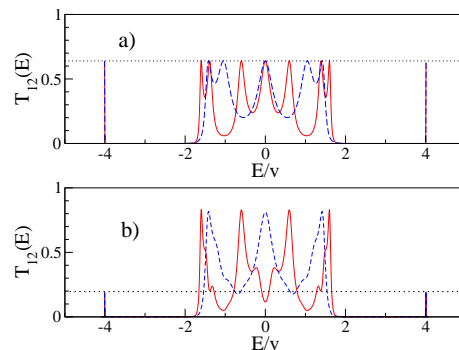


Figure 3: (Color online) Transmission coefficients T_{12} as a function of energy, for $M = 4$, $t_1 = 3$, $t_2 = 2$, and $t_3 = t_4 = 1$. Full red curves stand for $\gamma = 0.6$, while dashed blue curves correspond to $\gamma = 5$. a) symmetric case $N = 4$; b) asymmetric case $N_1 = 4$, $N_2 = 4$, $N_3 = 3$, $N_4 = 5$. Horizontal dotted lines are the theoretical results given by Eq. (15) and its generalization to unequal branch lengths.

Of special interest is the value of the transmission coefficient T_{ab} for the resonances outside the band. Since these resonances are very narrow, one can estimate $T_{ab}(\mathcal{E}_{\text{loc}})$ [16, 24] in terms of the edge components of the localized state ψ_{loc} in channels a and b ,

$$T_{ab}(\mathcal{E}_{\text{loc}}) = \left| \frac{\langle a, N_a | \psi_{\text{loc}} \rangle \sqrt{\gamma} \langle \psi_{\text{loc}} | b, N_b \rangle \sqrt{\gamma}}{(i/2)\Gamma_{\text{loc}}} \right|^2. \quad (13)$$

which can be computed from Eqs (6, 7):

$$|\langle a, N_a | \psi_{\text{loc}} \rangle|^2 = |C_0|^2 t_a^2 e^{-N_a/\xi} \prod_{n=1}^{N_a-1} \mathcal{B}_n(Q, N_a). \quad (14)$$

In the special case of equal-length branches this result assumes the particularly simple Hauser-Feshbach form:

$$T_{ab}(\mathcal{E}_{\text{loc}}) = \frac{4t_a^2 t_b^2}{Q^2}, \quad a \neq b. \quad (15)$$

This relation is in good agreement with the data of Fig. 3a, as indicated by the dotted horizontal line. The value of $T_{ab}(\mathcal{E}_{\text{loc}})$ for narrow resonances depends on the hopping elements t_a only, and is independent of the coupling strength γ for equal values of the couplings, $\gamma_a = \gamma$. The numerical data also indicate that, for equal-length branches, the maximal value of the transmission coefficient for $|E| < 2$ is given by the same expression (15), while this does not happen when branches have different length, see Fig. 3 b). As $\gamma \rightarrow 0$, the lifetime of the localized states becomes very long.

INTRODUCING DISORDER

A key consideration in important practical applications is the influence of disorder. For this reason we study the circuit with diagonal disorder by adding the term V ,

$$V = \sum_a \sum_n \epsilon_{a,n} |a, n\rangle \langle a, n|, \quad (16)$$

to the non-Hermitian Hamiltonian (10). Here the site energies $\epsilon_{a,n}$ are random numbers uniformly distributed in the interval $[-W/2, W/2]$. According to the theory of disordered systems, for $N \rightarrow \infty$ all states within the energy band become exponentially localized with a localization length $\propto (v/W)^2$. For the isolated localized states, a weaker dependence on disorder can be expected, and it is more convenient to define a localization length ℓ_{loc} through the inverse participation number,

$$\ell_{\text{loc}} = \left(|\langle 0 | \psi_{\text{loc}} \rangle|^4 + \sum_{a=1}^M \sum_{n=1}^N |\langle a, n | \psi_{\text{loc}} \rangle|^4 \right)^{-1}. \quad (17)$$

Without disorder and for large N , the value of ℓ_{loc} for the isolated states can be estimated as

$$\ell_{\text{loc}} \approx \frac{4Q(Q-1)^2}{(Q-2) \left[Q(Q-2) + \sum_{a=1}^M t_a^4 \right]}. \quad (18)$$

Numerical data confirm that the isolated states are not affected by disorder up to a critical disorder strength, W_{cr} , that can be very large. Above W_{cr} , the localization length of the isolated states also begins to decrease. This

critical value can be estimated by assuming that it corresponds to the intersection between the gap of size Δ emerging due to disorder around the localized states and the bulk of the spectrum of width $2(2v + W/2)$. One can estimate the value of Δ from the relation,

$$\Delta^2 = \overline{\langle \psi_{\text{loc}} | V | \psi_{\text{loc}} \rangle^2} = \frac{W^2}{12} \ell_{\text{loc}}^{-1}, \quad (19)$$

where the average is taken over sites n and over the disorder. The critical value W_{cr} for large N is thus obtained by equating the half-width of the density of states ($2v + W/2$) to the minimal possible energy of the isolated states due to random fluctuations:

$$\frac{Qv}{\sqrt{Q-1}} - \Delta \approx 2v + \frac{W}{2}, \quad (20)$$

which yields

$$W_{\text{cr}} = 2v \left(\frac{Q}{\sqrt{Q-1}} - 2 \right) \times \left(1 + \sqrt{\frac{(Q-2) \left[Q(Q-2) + \sum_{a=1}^M t_a^4 \right]}{12Q(Q-1)^2}} \right)^{-1}. \quad (21)$$

Despite the cumbersome appearance of Eq. (21), it admits two interesting limits: assuming for simplicity $t_a = t$ for all a , it is easy to see that for $Q \approx 2$, $W_{\text{cr}}/v \simeq (Q-2)^2/2$, while for $Q \rightarrow \infty$, one has $W_{\text{cr}}/v \simeq k\sqrt{Q}$, where the constant $k = 2/(1 + \sqrt{(M+1)/(12M)})$ depends only on the number of branches, and $k \approx 1.55$ for large M . Note that it is impossible to have delocalized isolated states along with localized states inside the band for any disorder W . The expression (21) is compared with numerical data for W_{cr} defined as the point where the localization length ℓ_{loc} of the isolated localized state begins to decrease with an increase of disorder. The data in Fig. 4 show quite good agreement with this estimate over many orders of magnitude with no fitting parameters.

SUMMARY

As an example of a non-trivial quantum network, we have studied the properties of an open circuit with M branches coupled to each other through one common point. The transmission properties of the open model were studied in relation to the structure of the energy spectrum and eigenfunctions of the parent closed system. The method of the effective non-Hermitian Hamiltonian allows one to derive the exact solution of the problem. Our main interest was in the energies and localization lengths of special eigenstates located outside the crystal energy band and strongly localized at the junction. It

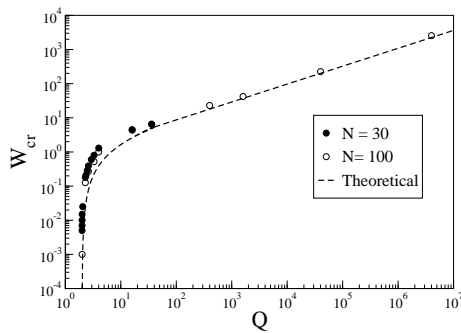


Figure 4: Critical value W_{cr} in units where $v = 1$, as a function of $Q = \sum_a t_a^2$ for $M = 4$. We choose for simplicity $t_a = t$ for $a = 1, \dots, M$, so that $Q = Mt^2$. Circles represent numerical data (full $N = 30$, open $N = 100$), while the dashed line shows the prediction (21).

was shown that, in the presence of coupling to the continuum, these states typically become narrow resonances with a very large lifetime. This fact may be important for the fabrication of new kinds of electron nanostructures, waveguides, antennas, and lasing devices with a large quality factor. Another possible application of the M -branch circuits follows from the expression (15), which points out the possibility of controlling and distributing energy incoming via one branch into all others. We have also shown the negligible influence of disorder in the branches on these special eigenstates. In our consideration the continuum coupling γ was taken as a constant parameter. In real arrangements, the circuit can be connected to transmitters or particle reservoirs. Then γ can depend on the signal energy and density of states in the reservoirs. Along with that, the continuum coupling will acquire a real part (dispersive integral) that should be added to the intrinsic Hamiltonian in Eq. (10). We hope to consider this more complicated situation elsewhere.

G.L.C is grateful to H. Pastawski for useful discussions. This work has been supported by Regione Lombardia and CILEA Consortium through a LISA Initiative (Laboratory for Interdisciplinary Advanced Simulation) 2011 grant [link: <http://lisa.cilea.it>]. This work was supported in part by the NSF under Grants No. PHY-0758099, PHY-1068217, and PHY-0545390. F.M.I. is thankful to VIEP of the BUAP (Puebla, Mexico) for financial support. Support by the grant D.2.2 2010 (Calcolo ad alte prestazioni) from Università Cat-

tolica is also acknowledged.

-
- [1] R. Hanson, L. P. Kouwenhoven, J. R. Petta, S. Tarucha, and L. M. K. Vandersypen, *Rev. Mod. Phys.* **79**, 1217 (2007).
 - [2] S. Kitavittaya, A. Rastelli, and O. G. Schmidt, *Rep. Prog. Phys.* **72**, 046502 (2009).
 - [3] G. Granger *et al.*, *Phys. Rev. B* **82**, 075304 (2010).
 - [4] P. Reberntrost, M. Mohseni, I. Kassal, S. Lloyd, and A. Aspuru-Guzik, *New J. Phys.* **11**, 033003 (2009).
 - [5] G. C. Solomon *et al.*, *J. Chem. Phys.* **129**, 054701 (2008).
 - [6] T. A. Fulton *et al.*, *Phys. Rev. Lett.* **63**, 1307 (1989).
 - [7] L. F. Santos and M. I. Dykman, *Phys. Rev. B* **68**, 214410 (2003).
 - [8] D. Giuliano and P. Sodano, *Nucl. Phys.* **B811**, 395 (2009).
 - [9] M. V. Feigel'man, L. B. Ioffe, V. B. Geshkenbein, P. Dayal, and G. Blatter, *Phys. Rev. B* **70**, 224524 (2004).
 - [10] C. A. Stafford, D. M. Cardamone, and S. Mazumdar, *Nanotechnology* **18**, 424014 (2007).
 - [11] H. Yan *et al.*, *Nature* **470**, 240 (2011).
 - [12] F.P. Mancini, P. Sodano, and A. Trombettoni, *Int. J. Mod. Phys. B* **21**, 1923 (2007).
 - [13] G. L. Celardo, A. M. Smith, S. Sorathia, V. G. Zelevinsky, R. A. Sen'kov, and L. Kaplan, *Phys. Rev. B* **82**, 165437 (2010).
 - [14] B. Bellazzini, M. Mintchev, and P. Sorba, *Phys. Rev. B* **80**, 245441 (2009).
 - [15] V. V. Sokolov and V. G. Zelevinsky, *Nucl. Phys.* **A504**, 562 (1989).
 - [16] V. V. Sokolov and V. G. Zelevinsky, *Ann. Phys. (N.Y.)* **216**, 323 (1992).
 - [17] A. F. Sadreev and I. Rotter, *J. Phys. A* **36**, 11413 (2003).
 - [18] A. Volya and V. Zelevinsky, *AIP Conference Proceedings* **777**, 229 (2005).
 - [19] S. Sorathia, F. M. Izrailev, G. L. Celardo, V. G. Zelevinsky, and G. P. Berman, *EPL* **88**, 27003 (2009).
 - [20] G. L. Celardo and L. Kaplan, *Phys. Rev. B* **79**, 155108 (2010).
 - [21] N. Auerbach and V. Zelevinsky, *Rep. Prog. Phys.* **74**, 106301 (2011).
 - [22] I. Brunelli, G. Giusiano, F.P. Mancini, P. Sodano, and A. Trombettoni, *J. Phys. B* **37**, S275 (2004).
 - [23] J. L. D'Amato, H. M. Pastawski, and J. F. Weisz, *Phys. Rev. B* **39**, 3554 (1989); H. M. Pastawski and E. Medina, *Rev. Mex. Fis.* **47**, 1 (2001).
 - [24] A. Ziletti, Master's Thesis, Università Cattolica, Brescia, Italy (2011), arXiv:1109.0727v1 [cond-mat.stat-mech].